Transient Foam Flow in Porous Media: Experiments and Simulation

*** Fergui O., * Quintard M., * Bertin H., ** Defives D.**

* LEPT - ENSAM, France

** IFP, France

ABSTRACT

Gas injection in the form of foam is an excellent way to enhance gas mobility control and overcome problems caused by density differences encountered during IOR operations.

Many studies have been developed to investigate the influence of experimental conditions (surfactant concentration and formulation, gas velocity, ...) on the foam displacement efficiency. However, these studies have mainly focused upon steady-state behaviour instead of transient aspects.

The experimental apparatus developed for this study is classical for this kind of investigation with the addition of saturation measurements using γ-rays attenuation technique. Our experiments were analysed in terms of breakthrough time, liquid recovery, differential pressure at breakthrough, gas saturation fields and trapped gas saturation. Our results show, in the absence of residual oil, a breakthrough time and a liquid recovery that increase with surfactant concentration.

The experiments were interpreted using a foam simulator including a classical Darcy's law model coupled with a foam bubble population balance equation taking into account generation, coalescence and convection of gas bubbles along the porous medium. Correlations for generation and coalescence of foam lamellae have been established according to the literature. We found that better agreement can be achieved between theoretical and experimental data with the full version of the Population Balance Model (PBM) than with a classical reservoir simulator. Difficulties associated with the estimate of the several parameters involved in the model are discussed.

References and illustrations at end of paper

1 INTRODUCTION

Foams are gas bubbles in liquids, in petroleum engineering it can be used as mobility control for IOR operations or as a barrier to reduce gas production in oil wells (Hanssen and Haugun, 1991).

Since the first studies by Bond and Holbrook (1958) and Fried (1961) many authors tried to understand and describe the foam generation, stability and propagation in porous media. Experimental studies performed with capillary tubes (Hirasaki and Lawson, 1985) or micromodels (Owete and Brigham, 1987) provide very exhaustive results concerning the foam nature and rheological behaviour in model porous media, but these results are not always representative of what happens really in a natural porous medium during an IOR process. Therefore, several authors studied foam in porous media, bead packs, sand, sandtone, (Huh and Handy, 1989; Llave et al., 1990) and focused on the steady-state determination of relative permeability curves. The main conclusions was that relative permeability to water was almost independent of the presence of surfactant, but, relative permeability to gas was significantly decreased in presence of surfactant. These results are difficult to be implemented for real case studies due to the unsteady-state behaviour of IOR processes. More recently, Kovsek and Radke (1993) reported unsteady-state results that could be described satisfactorily by a numerical model including a population balance equation.

In our study we consider the unsteady flow of foam in unconsolidated porous media in the absence of oil. We understand clearly that this last condition is not realistic for IOR operations, but, we believe that it is important to undestand the foam flow in the pore space before complicating the problem with the foam/oil interaction.

Our experiments were performed in a classical petrophysical way, measuring the breakthrough time, the evolution of the recovery, the pressure drop and the saturation fields during the foam flow.

The experiments were tentatively interpreted unsing a classical two-phase flow model with relative permeability curves being the best estimates we could get from the actual data. The agreement was poor, especially after breakthrough. In a second tentative, we used a foam simulator including a classical reservoir simulator coupled with a foam bubble population balance equation taking into account generation, coalescence and convection of gas bubbles.

2 EXPERIMENT

2.1 Experimental set-up

The experimental set-up, represented in Figure 1 was designed to perform foam flow in porous media at ambient pressure and temperature.

The gas (Nitrogen) was injected in the porous medium through a mass-flow controller allowing low values of the gas flow-rate (0 - 5 ml/min). The porous medium was made from calibrated sand (average diameter of particles = 74 10^{-6}m), packed in a parrallelepipedic cell (Length = 0.2 m, Cross Section Area = 0.002025 m^2) built of an inert material to avoid adsorption and reaction with the surfactant. The porosity was 0.4, the permeability 4 Darcy, and the total pore volume was around 160 cc.

During the foam flow, the saturation fields were measured using a γ-rays attenuation technique. This apparatus is made of a γ emittor (Am^{241}, activity = 435 mCi) coupled with a scintillator counter and photo-multiplicator. The set is moved by a 2-D displacement apparatus. Counting is performed by a Canberra™ multi-channel. The principle of the measurement is based on the Beer's law,

$$N = N_0 e^{-\zeta L} \qquad (1)$$

Where N is the counting, N_0 the reference counting, ζ the attenuation coefficient and L the width of the medium. The saturation was measured at several points of a net (grid represented in Figure 1) using the following equation (where the gas attenuation is neglected)

$$S_w = \frac{1}{L\varepsilon\zeta_w} \mathrm{Ln}\left(\frac{N}{N_w}\right) + 1 \qquad (2)$$

where ε is the porosity at the measurement location, ζ_w the attenuation coefficient of water and N_w is the counting measured at the considered point when the medium is 100 % water saturated. For our experimental device, we determined the saturations at 60 points (4

x 15). The counting time (20 S/point) allowed to performed a complete saturation map for less than 30 minutes. The injection rate (0.5 ml/min) was low enough to consider that the saturation map could be considered as an instantaneous picture. The pressure drop and water recovery were measured continuously using a differential pressure transducer (0 -150 mbar from H.B.M.™) and a precision weighing machine (0.01 g from Mettler™). A P.C. controlled the displacement apparatus, the photons counting and recorded all the data.

2.2 Procedure

The surfactant used in this study was an α-olefine sulfonate (C_{12} - C_{14}). The critical micellar concentration (CMC) was measured and found equal to 0.17% (mass fraction). The evolution of the interfacial tension as a function of surfactant concentration is given in Figure 2.

The water was deionized and deaerated before adding the surfactant.

The porous medium, placed vertically to avoid buoyancy effects, was saturated under vacuum, then flushed by the foaming solution to equilibrate the adsorption of surfactant molecules on the pore walls. This adsorption was considered to be achieved after the time necessary to injecte two pore volumes .

2.3 Experimental results

We performed several experiments to investigate the effect of surfactant concentration. The results are presented in term of recovery curve, pressure drop and saturation profiles.

The surfactant concentration values (mass fraction) are 0.05%, 0.1%, 0.17%, 0.3%, 0.4%, 0.5% and 1%. The injection flow rate of 0.5 ml/min corresponds to a Darcy velocity of 0.29 m/Day. The breakthrough times and final recoveries are plotted in Figure 3.

We observe an increase of the break-throug time (B.T.) until a concentration of 0.3% is reached, then a slight decrease. The increase is attributed to the modification of the mobility ratio and, in a minor way, to the decrease of interfacial tension driving a decrease of the capillary pressure. The final recovery increases rapidly when adding surfactant in the water and stays quite constant when we increase significantly the surfactant concentration.

The evolution of the pressure drops, reported in Fig.s 4, 5 and 6, can be annalysed in the following way : (i) the rapid increase of the pressure corresponds to foam generation at the entrance of the medium, (ii) then foam propagation leads to a slight increase of the pressure drop untill breakthrough. Subsequently, a quasi-steady state is reached. Differences due to surfactant concentration levels are discussed below. For surfactant concentration C = 0.05% and 0.1% behaviours are the same except in terms of breakthrough time. For the CMC concentration (0.17%) there is a sharp decrease of the pressure drop during the foam propagation stage, while pressure drops level remains the same after breakthrough.

Pressure drops, breakthrough times and whole behaviours are similar for mass fractions int he range 0.17% to 0.4%. This behaviour is characteristic of a displacement with strong mobility control.

For mass concentrations above 0.4%, the behaviour starts to change : (i) lower pressure drop before breakthrough, (ii) pressure drop increasing with concentration after breakthrough.

The "excess" of surfactant leads to a weaker mobility control before breakthrough for reasons that are not clearly identified. After breakthrough, there is still some water mobilization which is associated with a higher pressure drop by comparison to lower concentrations. This observation is confirmed by the saturation fields represented in Figures 7 and 8. For a surfactant concentration lower than 0.4% (Figure 7), there is no significative modification after the breakthrough. But, for C greater than 0.5% (Figure 8) we observe a modification of the saturation profiles corresponding to a propagation of foam that continue after the gas breakthrough.

3 FOAM DISPLACEMENT MODELLING

There are several models in the literature dedicated to the foam modelling in porous media. The most simple way consists in drawing up an experimental correlation between the gas mobility and the factors influencing it (namely the surfactant concentration, the gas velocity, the saturation, the permeability) (Islam and Farouq Ali, 1990). Then the flow is simulated introducing this correlation in a classical simulator. This way is quite easy to implement but does not take into consideration the complexity of the foam flow (generation and coalescence of bubbles).

More recently, Fisher et al. (1990), Rossen and Zhou (1992) developped models based on the existence of a critical capillary pressure corresponding to the lower value allowing foam generation. If we know the limit capillary pressure value we can fix the saturation corresponding and then solve the equation system using the fractional flow theory.

Patzek (1988), Friedman et al. (1988) applied the concept of population balance to foam flow. The idea is to write a population balance equation to describe the generation and coalescence of bubbles flowing inside the porous medium. In this model, gas mobility becomes a function of the lamellae population.

3.1 Population Balance Model (P.B.M)

The creation and destruction of gas bubbles are a function of gas velocity, capillary pressure and density of flowing lamellae.

The population balance equation can be written in the following form (Patzek, 1988),

$$\varepsilon S_g \frac{\partial}{\partial t}\left[x_f n_f + (1-x_f) n_t\right] + \nabla.(n_f u_g) = \varepsilon S_g \left[G_f(v_g) - C_f(n_f, P_c, v_g)\right] \quad (3)$$

Where S_g is the gas saturation, G_f is the bubble generation term, C_f is the coalescence term, x_f is the gas flowing fraction, n_f is the flowing lamellae density and n_t is the total lamellae density. u_g is the darcy velocity of gas, v_g is the interstitial gas velocity. As reported in the literature, G_f is a function of the local gas velocity only, whereas the coalescence rate is a function of the gas velocity, the capillary pressure and the number of flowing lamellae. In Eq. 3 many terms must be computed using correlations developped in the literature. These correlations are reported in the papers of Friedmann et al. (1988), Chang et al. (1990) and Kovsek and Radke (1994). Considering the results obtained in the last paper, we choose to take similar correlations :

- gas flowing fraction

$$x_f = \text{constant} \quad (4)$$

- Lamellae generation

The lamellae are generated by snap-off or leave-behind phenomena, the main parameters influencing the generation are the interstitial gas and water velocities

$$G_f = k_g v_g^{1/3} v_w \quad (5)$$

where k_g is the generation parameter

- Coalescence term

The coalescence of two bubbles is mainly due to:

  * gas diffusion
  * lamellae breaking,

it will be proportional to the interstitial gas velocity and the flowing lamellae density,

$$C_f = k_c v_g n_f \quad (6)$$

where k_c, the coalescence parameter, is defined in the following way,

$$k_c = k_c^0 \left(\frac{1-S_w}{1-S_w^*}\right) \quad (7)$$

where S_w^* is the critical water saturation corresponding to the critical capillary pressure (Khatib et al., 1988).

- foam viscosity

The viscosity of the foam (μ_f) depends on :

  * the density of mobile lamellae
  * the gas velocity

$$\mu_f = \mu_g + \frac{\alpha n_f}{v_g^{1/3}} \quad (8)$$

where α is a viscosity parameter function of the permeability.

The conservation equation are written in the following way,

$$\frac{\partial}{\partial t}(\varepsilon S_w \rho_w) + \nabla.(\mathbf{u}_w \rho_w) = 0 \qquad (9)$$

$$\frac{\partial}{\partial t}(\varepsilon S_g \rho_g) + \nabla.(\mathbf{u}_g \rho_g) = 0 \qquad (10)$$

where S_w ,ρ_w and $\mathbf{u}_w$ are the water, saturation, density and darcy velocity. Similar definitions applied for the gas phase.

The generalized Darcy's laws are :

$$\mathbf{u}_w = -\frac{k_{rw}}{\mu_w}\mathbf{K}.(\nabla P_w - \rho_w g) \qquad (11)$$

$$\mathbf{u}_g = -\frac{k_{rg}}{\mu_g}\mathbf{K}.(\nabla P_g - \rho_g g) \qquad (12)$$

$\mathbf{K}$ is the effective permeability, k_{rw} and k_{rg} are the relative permeabilities of water and gas. P_w and P_g are the water and gas pressures.

The relative permeabilities are expressed in Corey's form

$$k_{rw} = k_{rw}^0 \left[\frac{S_w - S_{wr}}{1 - S_{wr}}\right]^n \qquad (13)$$

$$k_{rg} = k_{rg}^0 \left[1 - \frac{S_w - S_{wr}}{1 - S_{wr}}\right]^n \qquad (14)$$

Where S_{wr} is the residual water saturation (after gas drainage).

In addition, we consider that the relative permeability to the gas in presence of foam is a function of the relative permeability to gas in absence of foam through the flowing gas fraction,

$$k_{rg}^f(S_g) = x_f k_{rg}(S_g) \qquad (15)$$

The system of equations is completed by the capillary pressure relation

$$P_c = P_g - P_w \qquad (16)$$

which can be expressed, by using the Leverett function,

$$Pc = \sigma(C)\left(\frac{\varepsilon}{K}\right)^{1/2}\left(\frac{0.067}{S_w - S_{wr}}\right)^{0.2} \qquad (16)$$

Where σ is the interfacial tension.

In the case of injection of a surfactant slug, we have to write a dispersion equation to express the surfactant concentration evolution,

$$\varepsilon\frac{\partial}{\partial t}(S_w C) + \nabla.(\mathbf{u}_w C) = \nabla.(\mathbf{D}\nabla C) \qquad (17)$$

Where C is the surfactant mass concentration and D the dispersion coefficient.

The general problem is written in 1D, the flow of the two fluids was specified at the inlet side (constant value of the gas flow-rate, no water flow) and the capillary pressure was maintened at zero at the outlet side.

$$q_g = q_o \text{ at } x = 0 \qquad (18)$$

$$P_c = 0 \text{ at } x = L \qquad (19)$$

The mathematical model is solved using the IMPES method (Aziz and Settari, 1979). The main difficulty is the choice of the values of the different parameters appearing in the correlations.

First, the Corey's coefficients were determined by matching a water-gas displacement experiment, we found :

$k_{rg}^0 = 0.7$

$n = 3.$

According to the experiments the residual water saturation is fixed to

$S_{wr} = 0.1$

The following parameters occuring in the population balance model were determined according to literature results (Friedmann et al.,1988; Kovsek and Radke, 1994),

$x_f = 0.1$

$\alpha = 1.10^{-13}$

$k_g = 1.10^{-8}$

$k_c = 1.$

In addition we fixed the value of the critical water saturation (corresponding to the critical capillary pressure),

$S_w^* = 0.01$

3.2 Numerical simulations

Figures 9 and 10 represent the experimental saturation and pressure drop curves compared to the simulated results. The numerical saturation fits correctly the experimental results. In Figure 10 we observe a difference in terms of the amplitude of pressure drops but the whole behaviour (foam propagation, breakthrough, equilibrium) is qualitatively well described.

In addition to these numerical results we plotted in Figure 11 the evolution of the density of mobile lamellae as a function of the location. We observe that n_f increases faster as we get closer the outlet of the medium. This is due to the propagation (convection/advection) of the mobile lamellaes, and to that we are always in a generation state (the critical capillary pressure was taken high enough). This latter condition can be modified if we choose a lower level of the critical capillary pressure, that will increase the value of the critical saturation.

In the following section we investigate the influence of the different parameters on the gas mobility (flowing gas fraction, foam texture and critical capillary pressure).

Influence of the gas flowing fraction

In Figure 12 we plotted the pressure drops computed for different values of x_f.

The increase of x_f leads to :

* a decrease of the slope of the propagation stage
* a decrease of the breakthrough time
* a decrease of the finak pressure drop.

Influence of generation/coalescence ratio

We fixed a value of k_g equal to 1 and varied the value of k_c. These two parameters are important for the foam modelling because they can take into account the effect of the modification of the surfactant concentration through the ratio generation/coalescence. The pressure drop is very sensitive to this ratio as represented in Figure 13. The density of mobile lamellaes is, of course, very sensitive to the parameters.

Influence of the critical capillary pressure

This value occurs, *via* the critical water saturation in the coalescence correlation (Eq. 7).

The influence of this parameter on the evolution of the mobile lamellae density as a function of the location is showed in Figure 14 (the curves are plotted for 0.5 Pore Volume of injected gas). The maximum of lamellae density is obtained for low values of the critical water saturation (high value of P_c).

4 CONCLUSION

We performed an experimental and numerical study on transient foam flow in porous media in the absence of oil. The main conclusions of this study are :

1.) The experiments show clearly the influence of the surfactant concentration on the gas mobility. The shapes of the pressure drop and saturation profiles are slightly different according to the surfactant concentration.

2.) The modelling of transient foam flow using a population balance equation provides interesting results but the parameters in the correlations are numerous and not easy to determine.

ACKNOWLEDGEMENTS:
We gratefully acknowledge Institut Français du Pétrole and Ecole Nationale Supérieure du Pétrole et des Moteurs, who supported this work and sponsored O. Fergui during his stay in the laboratory.

REFERENCES

Aziz K. and Settari A., Petroleum Reservoir Simulation, Applied Science Publishers Ltd, London, 1979

Bond D.C. and Holbrook O.C.: Gas drive oil recovery process, U.S. Patent N° 2,866,507, 1958.

Chang S.H., Owusu L.A., French S.B. and Kovarik F.S.: The effect of microscopic heterogeneity on CO_2 foam mobility : part 2 Mechanistic foam simulation. Paper SPE 20191 presented at the SPE/DOE Enhance Oil Recovery Symposium, Tulsa, OK, April 22-25, 1990.

Fisher A.W., Foulser R.W.S. and Goodyear S.G.: Mathematical modeling of foam flooding. Paper SPE 20195 presented at the SPE/DOE Enhance Oil Recovery Symposium, Tulsa, OK, April 22-25, 1990.

Fried A. N.: Foam drive process for increasing the recovery of oil. Bureau of Mines Report of Investigation, 1961.

Friedman F., Chen W.H. and Gauglitz P.A.: Experimental and numerical study of high temperature foam displacement in porous media. Paper SPE 17357 presented at the SPE/DOE Enhance Oil Recovery Symposium, Tulsa, OK, April 17-20, 1988.

Hanssen J.E. and Haugun P.: Gas blockage by non-aqueous foams. Paper SPE 21002 presented at the international Symposium on Oilfield Chemistry, Anaheim, California, (Feb. 20-22), 1991.

Hirasaki G.J.and Lawson J.B.: Mechanisms of foam flow through porous media : Apparent viscosity in smooth capillaries. SPE J. (April) pp 176-190, 1985.

Huh D.G.and Handy L.L.: Comparison of steady and unsteady state flow of gas and foaming solution in porous media. SPE Res. Engng. (Feb.), p 77-84, 1989.

Islam M.R. and Farouq Ali S.M.: Numerical simulation of foam flow in porous media. J. Can. Petrol. Technol. (July-Aug.), pp 47-51, 1990

Khatib Z.I., Hirasaki, G.J. and Falls A.H.: Effects of capillary pressure on coalescence and phase mobilities in foams flowing through porous media. SPE Res. Engng.(Aug. 1988), pp 919-926, 1988.

Kovscek A.R. and Radke C.J.: A comprehensive description of transient foam flow in porous media. Paper DOE/NIPER presented at the Symposium on field application of foams for oil production, Bakersfield, California, Feb. 11-12, 1993.

Llave F.M., Chung F.T.H. Louvier R.W. and Hudgins D.A.: Foams as mobility control agents for oil recovery by gas displacement. Paper SPE 20245 presented at the SPE/DOE Enhance Oil Recovery Symposium, Tulsa, OK, April 22-25, 1990.

Owete S.O. and Brigham W.E.: Flow behavior of foam : a porous micromodel study. SPE Res. Engng. (Aug.1987), pp. 315-323, 1987.

Patzek T.W.: Description of foam flow in porous media by the population balance method. *in* Surfactant Based Mobility Control Progress in Miscible Flood Enhanced Oil Recovery. Smith D.H. Ed., ACS Symposium Series N° 373, 326-341, 1988.

Zhou Z.H. and Rossen W.R.: Applying fractionnal flow theory to foam processes at limiting capillary pressure. Paper SPE 24180 presented at the 8th SPE/DOE Symposium on Enhanced Oil Recovery, Tulsa, OK, Apr. 22-24, 1992.

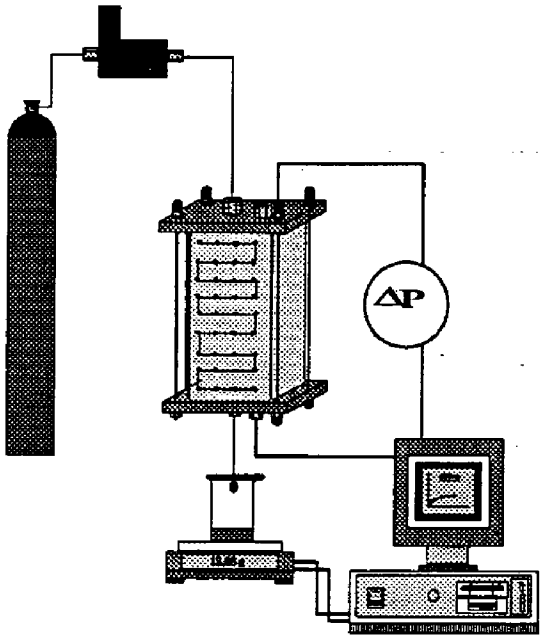

Figure 1 : Experimental Set-Up

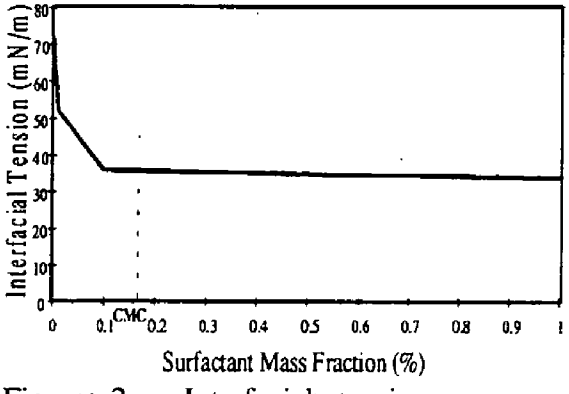

Figure 2 : Interfacial tension as a function of surfactant concentration

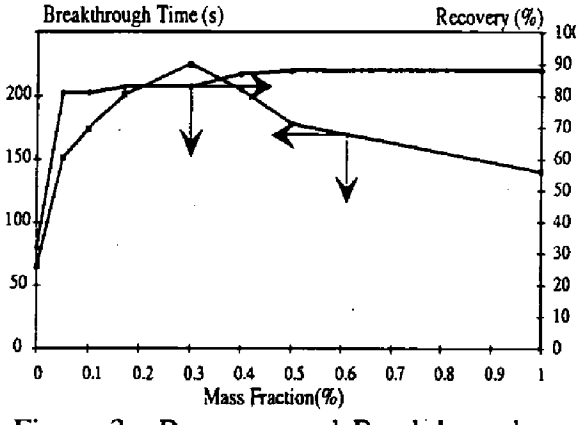

Figure 3 : Recovery and Breakthrough time as a function of surfactant concentration

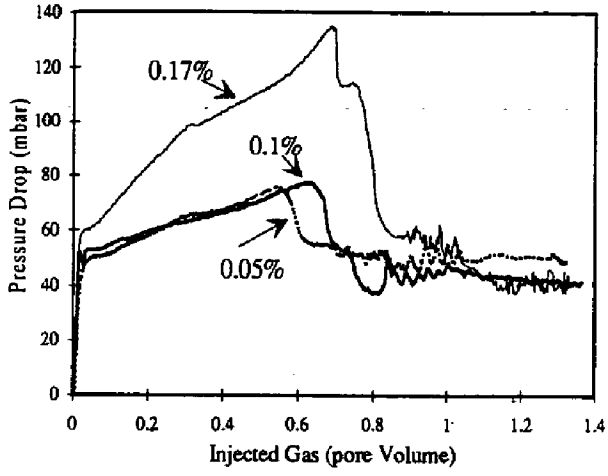

Figure 4 :Pressure Drop Curves
(0.05% < C < 0.17%)

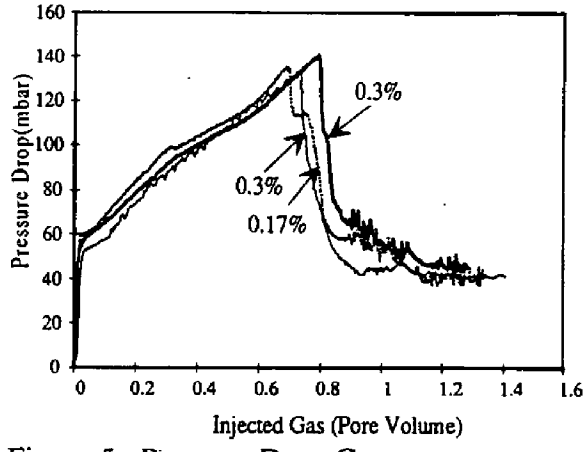

Figure 5 : Pressure Drop Curves
(0.17 % < C < 0.4%)

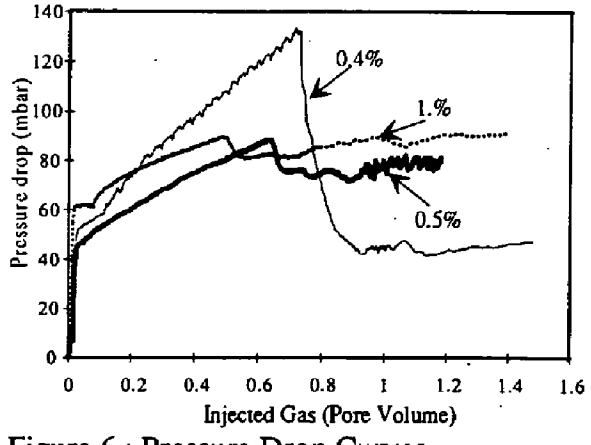

Figure 6 : Pressure Drop Curves
0.4 % < C < 1%

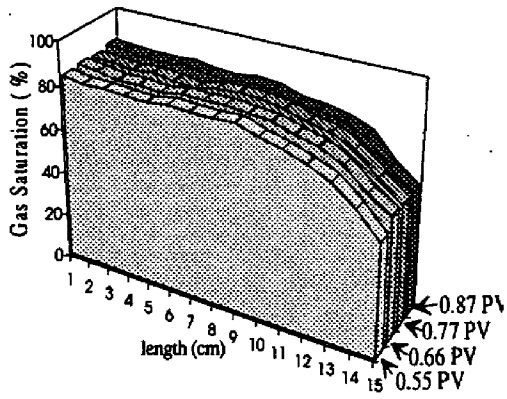

Figure 7 : Gas Saturation (C < 0.4%)

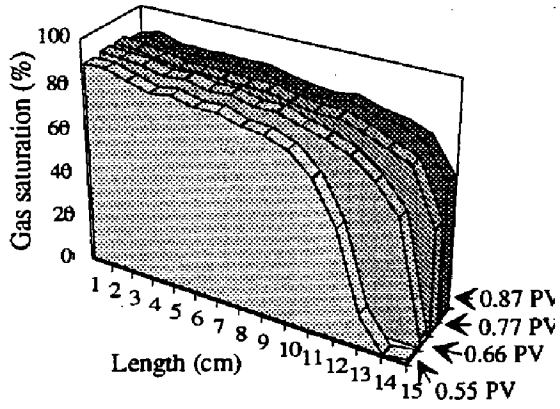

Figure 8 : Gas Saturation (C > 0.5%)

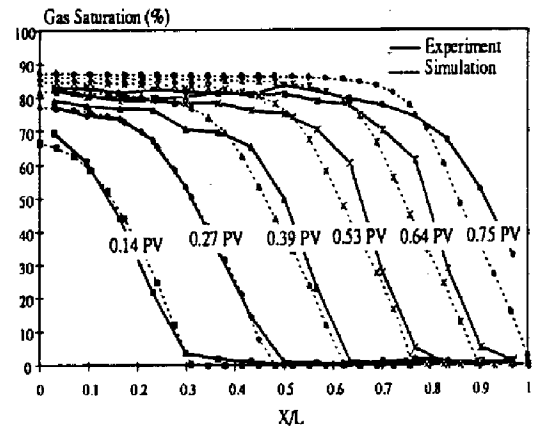

Figure 9 :Experimental and simulated Saturation Profiles

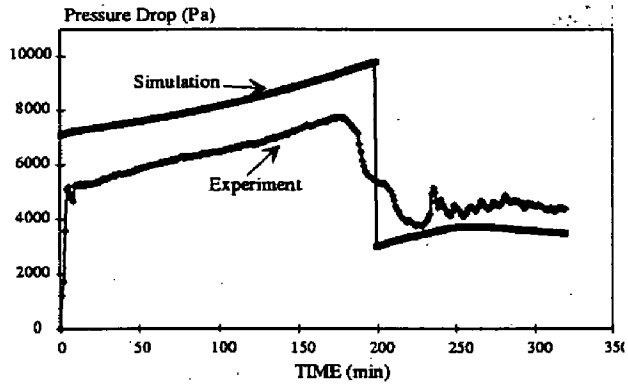

Figure 10 : Experimental and simulated Pressure Drops.

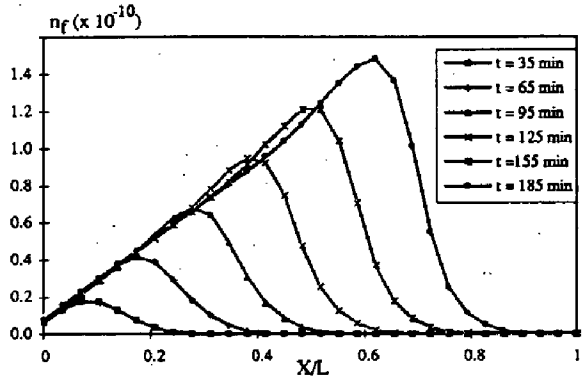

Figure 11 :Evolution of the density of mobile lamellaes.

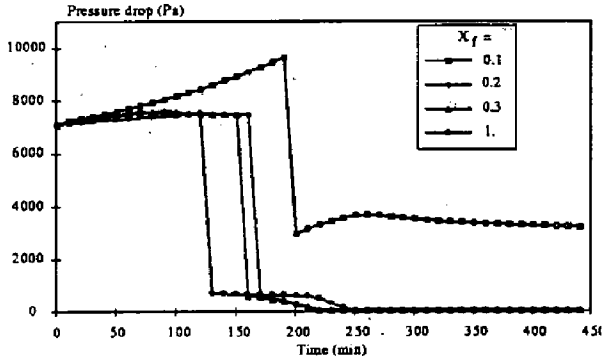

Figure 12 :Influence of the gas flowing fraction on the pressure drop.

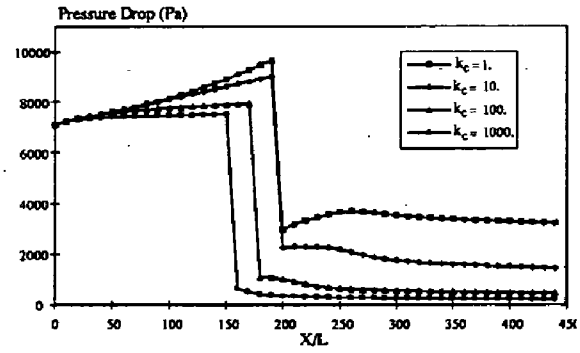

Figure 13 :Influence of the coalescence term on the pressure drop.

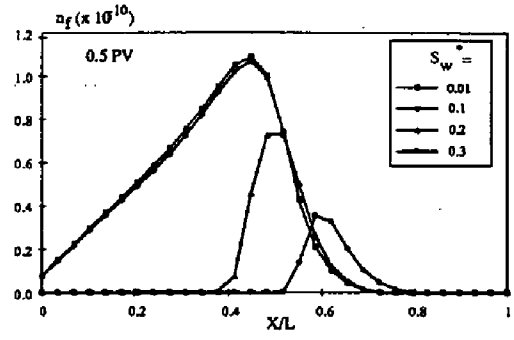

Figure 14 : Density of mobile lamellaes as a function of the critical water saturation (injected gas volume is equal to 0.5 PV)